

Supplementary Material Available: Tables of atomic coordinates, interatomic distances and angles, and thermal parameters and a figure showing a cyclic voltammetry scan (5 pages). Ordering information is given on any current masthead page.

Department of Chemistry
University of Virginia
Charlottesville, Virginia 22901

G. L. Lilley
E. Sinn
B. A. Averill*¹

Received November 18, 1985

High-Salt and Low-Salt Models for Kinked Adducts of *cis*-Diamminedichloroplatinum(II) with Oligonucleotide Duplexes

Sir:

DNA, the likely *in vivo* target of the anticancer drug *cis*-diamminedichloroplatinum(II) (*cis*-DDP), undergoes certain geometrical changes upon drug binding. There is general agreement that *cis*-DDP binds predominantly to d(GpG) units,¹ and following the recent crystal structure determination of the complex *cis*-[Pt(NH₃)₂d(pGpG)],² metrical parameters for the platinum-d(GpG) chelate have been provided. Details about the structural changes caused by *cis*-DDP binding to oligonucleotide duplexes and to DNA itself, however, are not yet available and are currently the subject of several theoretical and experimental investigations.

By using molecular mechanics calculations, we recently derived a model³ for the adduct of *cis*-[Pt(NH₃)₂]²⁺ with oligonucleotides that revealed disruption of GC base-pairing at the 5'-end-coordinated guanine of the platinum-cross-linked d(GpG) site, a switching of sugar pucker to C(3')-endo for the same 5'-guanosine, and a hydrogen bond between the coordinated ammine ligand and the 5'-phosphate group. The directionality of the helix axis, however, was largely unperturbed. In this study we have found two alternative models having comparable conformational energies where the helix axis is substantially kinked. These new results prove that kinking of DNA upon platination, as previously suggested,⁴ is energetically feasible and provide atomic coordinates for refined model structures of kinked *cis*-[Pt(NH₃)₂]²⁺-oligonucleotide adducts.

The kinked models were constructed by using coordinates from the platinated adduct (1) of the single-stranded hexanucleotide, d(AGGCCT), which, after energy refinement, showed a kink of approximately 67° (Figure 1).⁵ We started with the unplatinated, energy-refined B-DNA structure of the decanucleotide duplex investigated previously,³ [d(TCTCG*G*TCTC)-d(GAGACC-GAGA)] (2), where the asterisks designate the platinum binding sites, in which the sugar pucker of the 5'-G* guanosine was switched from C(2')-endo to C(3')-endo. The duplex was divided into two parts along the G*pG* site (dashed line in Chart I). Each of the G* designated guanine rings of 2 was then fit by a least-squares procedure into the appropriate guanine residue of the platinated hexanucleotide 1, so that the resultant kinked duplex had the same G*pG* fragment geometry as the single-stranded adduct 1. The *cis*-[Pt(NH₃)₂]²⁺ unit with coordinates from 1 was then added to the new coordinate file, yielding a kinked platinated

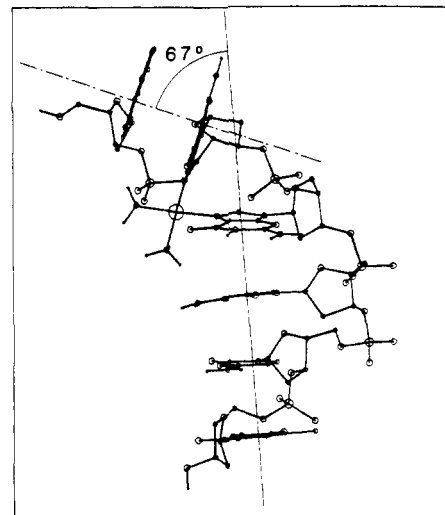


Figure 1. Side view of *cis*-[Pt(NH₃)₂]-[d(AGGCCT)-N7(2),N7(3)] (B-DNA model⁵ after energy minimization).

duplex. This duplex showed a gap at p16-C15 in the backbone of the unplatinated strand, with a P-O(3') bonding distance of ~10 Å. In order to reduce this distance and enable the energy-minimizing program AMBER⁷ to close the gap without destroying the kink, we subsequently rotated each duplex part about an axis passing through the coordinated N(7) atom and paralleling the helix axis of the rotated part, so that the P-O(3') distance was diminished. The factors limiting the extent of the rotations were the two cytosines base-paired with the central G*pG* unit, the amino groups of which would have clashed if the rotation were carried too far. The final P-O(3') distance at the site of the break was 4-5 Å. This distance could have been diminished even further by rotating the O(5')-P group at the 5'-side of the gap about the C(4')-C(5') bond. This adjustment was also easily accomplished by AMBER, and the outcome of the refinement did not depend on whether or not we had performed the latter rotation. Manual rotations were accomplished by using the computer graphics system FRODO PS-300.⁸ The resultant kinked structures were then refined with the program AMBER. In the first three cycles we constrained all base atoms to their positions with a penalty function $E = \sum k(\Delta r_i)^2$, where Δr_i are the shifts of the atoms from their initial sites, added to the total energy.⁷ The constant k was reduced from 100 to 10 kcal/(mol Å²) in the second step of refinement and finally to 1 kcal/(mol Å²). Subsequently, the constraint was completely removed and the structure refined again. The purpose of the constraint was to allow the backbone to adjust while the kinked structure of the duplex remained unchanged. This procedure of rotating the least-squares-fitted structure followed by energy minimization yielded two distinct models, identified as B and C in the following text in order to distinguish them from the uninked model A reported previously.³

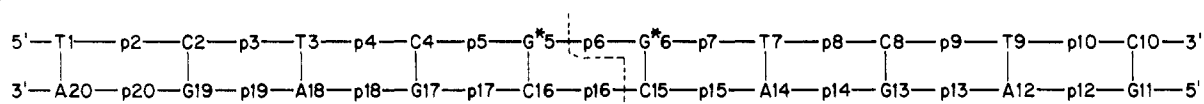
The AMBER refinements were carried out by using standard parameters.⁹ To examine the robustness of the solutions, several models for the environmental dielectric constant were used. While these models had a substantial effect on the magnitude of the energies, they had little effect on the relative energies or the resultant geometry. Here we report models and energies derived by using a dielectric constant of 4 r , where r is the internuclear separation, and with no additional shielding of 1-4 neighbors.

The refined structures showed a number of unusual backbone torsional angles at the site of kinking and an unexpected N-type

- (1) Pinto, A. L.; Lippard, S. J. *Biochim. Biophys. Acta* **1985**, *780*, 167-180.
- (2) Sherman, S. E.; Gibson, D.; Wang, A. H.-J.; Lippard, S. J. *Science (Washington, D.C.)* **1985**, *230*, 412-417.
- (3) Kozelka, J.; Petsko, G. A.; Quigley, G. J.; Lippard, S. J. *J. Am. Chem. Soc.* **1985**, *107*, 4079-4081.
- (4) (a) den Hartog, J. H. J.; Altona, C.; van Boom, J. H.; van der Marel, G. A.; Haasnoot, C. A. G.; Reedijk, J. J. *Biomol. Struct. Dyn.* **1985**, *2*, 1137-1155. (b) Miller, K. J.; Taylor, E. R.; Basch, H.; Krauss, M.; Stevens, W. J. *Ibid.* **1985**, *2*, 1157-1171. (c) Sundaralingam, M.; Rubin, J. R.; Rao, S. T. In "The Molecular Basis of Cancer, Part B: Macromolecular Recognition, Chemotherapy, and Immunology"; Rein, R., Ed.; A. R. Liss: New York, 1985; pp 175-184.
- (5) Kozelka, J.; Petsko, G. A.; Quigley, G. J.; Lippard, S. J., manuscript in preparation.
- (6) Arnott, S.; Campbell-Smith, P.; Chandrasekharan, P. "Handbook of Biochemistry and Molecular Biology", 3rd ed.; Fasman, G. D., Eds.; Chemical Rubber Co.: Cleveland, OH, 1976; Vol. 2, pp 411-414.

- (7) Weiner, P.; Kollman, P. J. *Comput. Chem.* **1981**, *2*, 287-303.
- (8) (a) Jones, T. A. In "Computational Crystallography"; Sayre, D., Ed.; Clarendon Press: Oxford, 1982; pp 303-317. (b) Pflugrath, J. W.; Saper, M. A.; Quijcho, F. A. In "New Generation Graphics System for Molecular Mechanics", presented at the International Summer School on Crystallographic Computing, Kyoto, Japan, 1983.
- (9) Weiner, S. J.; Kollman, P. A.; Case, D.; Singh, U. C.; Ghio, C.; Alagona, G.; Profeta, S., Jr.; Weiner, P. *J. Am. Chem. Soc.* **1984**, *106*, 765-784.

Chart I



conformation of the C4 cytidine deoxyribose ring. The backbone angles turned out to be artifacts derived from the "manual" bending procedure; restoring these torsional angles to their normal ranges lowered the energy. The N-conformation of cytidine C4, however, proved to be a distinctive feature of both models (Table I).^{10,11} In addition, both models had the N-conformation of guanosine G5, as was also found for unknicked models.³

Figure 2 shows stereoviews of models B and C. Both models bend toward the major groove, the helix axes subtending angles of 60° (B) and 50° (C), respectively. The interplanar angles between the two coordinated guanines (58.4° in B; 63.2° in C) do not differ appreciably from the value found in the unknicked model A (58.0°). A notable feature, however, is the angle formed between the planes of the bases C4 and G5, which was almost perpendicular in model A (86.4°) but, in the kinked models, assumes values of 30.1° (B) and 22.7° (C), respectively. This difference reflects the better base stacking within each separate part of the duplex in the latter two structures.

The kinked geometry, as well as the base stacking within both arms of models B and C, results in a favorable attraction between phosphate group p4 and the platinum residue, since kinking brings these two groups closer together. The Pt-P(p4) distance is 5.0 Å in B and 5.5 Å in C, compared to 10.0 Å in model A. The hydrogen bond between phosphate group p5 and one ammine ligand of platinum, a stabilizing feature of model A, also appears in models B and C. In addition, the same ammine ligand is hydrogen-bonded to the phosphate group p4. The formation of the hydrogen bond to p4 imposes a slightly unfavorable conformation on the deoxyribose ring of C4 (negative pseudorotation angle; see Table I), so that the net energy gain in forming this hydrogen bond is only 2–3 kcal/mol. Control refinements revealed the energy minimum to be very shallow with respect to the distance between platinum and phosphate p4. The most stable structures, which we report here, were achieved by constraining the distances Pt-P(p4) and Pt-P(p5) to 5.2 Å, refining, and then relaxing the constraints.

Base-pairing of G5 with C16 is impaired in model B. The hydrogen bond from the amino group of G5 is disrupted and the imino hydrogen bond weakened. In model C, on the other hand, all hydrogen bonds involved in base-pairing are intact. In both models, one ammine ligand of platinum forms a hydrogen bond to O(6) of G6. Hydrogen bonds from C4 and T7 to ammine ligands, present in model A,³ are absent in models B and C.

Detailed examination of the two kinked models revealed that residues 6–15 have very similar geometries, which can be superimposed with a root-mean-square deviation of the atomic shifts of only 0.45 Å. The main feature that distinguishes the kinked models from one another is the pronounced tipping of the 5' end of the platinated strand in model B (Figure 2), narrowing the opening to the crevice created by the kink and leading to short distances between phosphate groups p2 and p14 and between p3 and both p13 and p14 (P–P distances of 5.2, 4.9, and 6.3 Å, respectively). These phosphodiester groups are bridged by four sodium counterions (Figure 2a). When the bridging ions are removed and the energy reminimized with AMBER, the B structure refines toward a geometry similar to that of model C, with a wide opening to the crevice.

Model B is energetically favored over model C by 19.3 kcal/mol, the difference being entirely due to the interaction of the helix with the counterions. When the conformational energy is calculated for the helices alone (excluding the sodium ions), almost equal values result for all three models: A, –543.3 kcal/mol; B,

Table I. Structural Parameters for the Two Kinked Model Structures of *cis*-[Pt(NH₃)₂] Adducts of [d(TCTCGGTCTC)-d(GAGACCGAGA)-N7(5),N7(6)]^a

resi- due	ϕ	q	χ	α	β	γ	δ	ϵ	ζ
Model B									
T1	173	0.30	-114			57	142	-175	-86
C2	96	0.32	-126	-70	169	55	100	-176	-78
T3	146	0.40	-110	-67	171	56	136	-168	-154
C4	-11	0.37	-174	-77	177	41	91	-150	-71
G5	2	0.44	-155	-81	178	52	81	-132	-63
G6	145	0.31	-133	-60	-172	59	129	-175	-89
T7	139	0.37	-125	-66	176	55	128	-176	-122
C8	168	0.30	-119	-61	171	60	140	-178	-91
T9	120	0.33	-130	-67	173	57	114	-179	-88
C10	136	0.38	-119	-67	174	56	128		
G11	178	0.31	-116			57	145	-171	-85
A12	99	0.32	-126	-76	171	54	102	179	-85
G13	141	0.38	-125	-65	171	59	130	-179	-111
A14	174	0.31	-115	-65	-178	57	144	-172	-86
C15	96	0.33	-122	-75	169	55	100	-169	-88
C16	131	0.34	-119	-83	-178	52	122	-174	-84
G17	128	0.36	-123	-73	174	55	120	179	-89
A18	130	0.32	-121	-66	174	59	120	178	-91
G19	120	0.36	-126	-64	173	59	113	176	-90
A20	140	0.38	-122	-65	177	56	131		
Model C									
T1	171	0.32	-120			57	143	-172	-83
G2	113	0.35	-124	-74	172	54	109	-178	-84
T3	136	0.40	-119	-67	170	58	127	-177	-144
C4	-5	0.39	-163	-63	170	42	86	-154	-71
G5	0	0.40	-154	-66	168	56	86	-113	-68
G6	102	0.31	-136	-63	176	58	104	177	-92
T7	146	0.33	-122	-61	177	59	130	-177	-110
C8	160	0.32	-114	-65	173	60	138	179	-96
T9	132	0.33	-127	-66	175	57	121	-179	-92
C10	144	0.38	-118	-67	176	56	134		
G11	172	0.32	-120			58	143	-175	-89
A12	131	0.35	-121	-72	175	55	121	-180	-91
G13	128	0.38	-129	-67	174	58	119	177	-102
A14	166	0.33	-116	-66	-175	57	142	-175	-82
C15	68	0.36	-127	-78	176	47	85	-168	-77
C16	82	0.34	-132	-72	174	53	93	-177	-80
G17	144	0.36	-122	-64	168	60	130	176	-103
A18	160	0.31	-114	-63	-178	58	136	-179	-102
G19	136	0.35	-120	-66	174	58	125	179	-97
A20	150	0.37	-118	-67	177	56	138		

^a ϕ , q = phase and amplitude of pseudorotation of the deoxyribose ring;¹⁰ χ = torsional angle along the glycosidic bond; α – ζ = torsional angles along the backbone.¹¹ All angles are in degrees; q is in angstroms.

–543.1 kcal/mol; C, –545.6 kcal/mol. Thus, all three models are comparable candidates to mimic oligonucleotide duplex adducts with *cis*-[Pt(NH₃)₂]²⁺.

Structural parameters for both kinked models are given in Table I. The local geometry around the platinum residue is in accord with crystallographic² and NMR^{4a,12a} work on platinated oligonucleotides. In particular, the 5'-coordinated guanosine features

(10) Cremer, D.; Pople, J. A. *J. Am. Chem. Soc.* **1975**, *97*, 1354–1358.

(11) Saenger, W. "Principles of Nucleic Acid Structure"; Springer-Verlag: New York, 1984; p 17.

(12) (a) den Hartog, J. H. J.; Altona, C.; van Boom, J. H.; van der Marel, G. A.; Haasnoot, C. A.; Reedijk, J. *J. Am. Chem. Soc.* **1984**, *106*, 1528–1530. (b) Van Hemelryck, B.; Guittet, E.; Chottard, G.; Girault, J. P.; Huynh-Dinh, T.; Lallemand, J. Y.; Igolen, J.; Chottard, J. C. *Ibid.* **1984**, *106*, 3037–3039. (c) den Hartog, J. H. J.; Altona, C.; Chottard, J. C.; Girault, J. P.; Lallemand, J. Y.; de Leeuw, F. A. A. M.; Marcellis, A. T. M.; Reedijk, J. *Nucleic Acids Res.* **1982**, *10*, 4715–4730. (d) den Hartog, J. H. J.; Altona, C.; van Boom, J. H.; Reedijk, J. *FEBS Lett.* **1984**, *176*, 393–397.

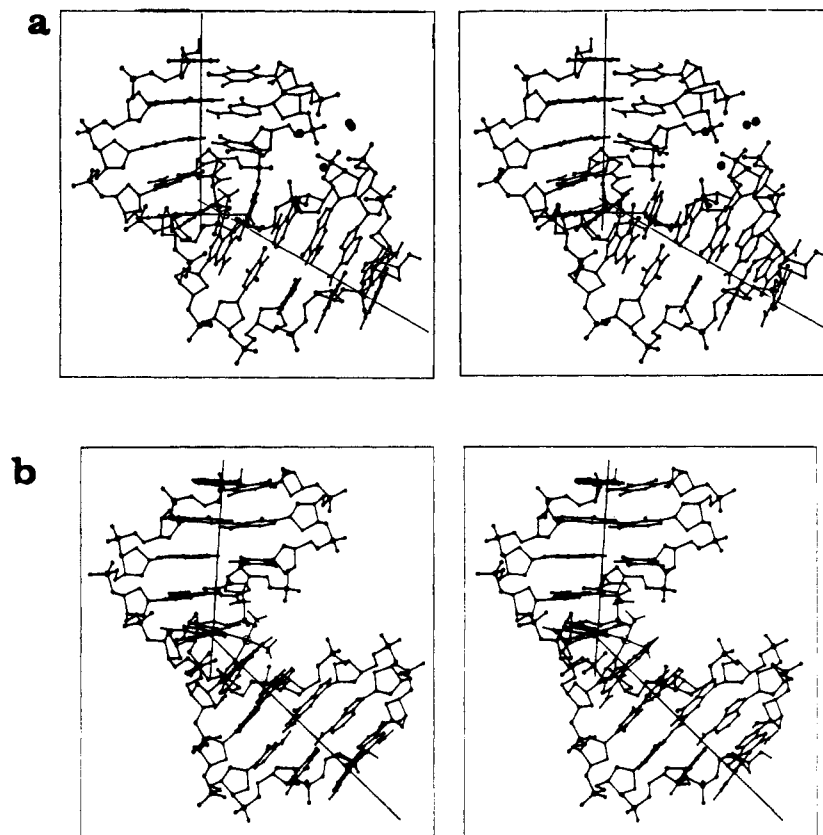


Figure 2. Stereoview of the two kinked models for $cis\text{-[Pt(NH}_3\text{)}_2\text{]}^{2+}$ adducts of $[\text{d(TCTCGGTCTC)-d(GAGACCGAGA)-N7(5),N7(6)}]$: (a) model B; (b) model C. Of the 16 sodium counterions used to compensate for the negative charge of the phosphates, only the four bridging ions stabilizing model B are shown. In both views, the 5' end of the platinated strand is pointing upward.

an N-type conformation of the sugar ring, which obviously helps to accommodate contraction of the backbone. Backbone contraction is further enhanced in the kinked models, leading in both models B and C to an O(4')-endo conformation of one or both cytidines base-paired with the central G*pG* unit (Table I). Finally, in both kinked models, the backbone contraction contributes to the S \rightarrow N repuckering on C4. The primary cause for this repuckering seems to be a short contact between the C(2') atom of C4 and one ammine ligand, an interaction that is removed when the sugar conformation changes from S- to N-type. The S:N sugar pucker sequence at the T3:C4 dinucleotide produces a relatively long distance of approximately 4.7 Å between the atoms C(3') of T3 and C(5') of C4. In unplatinated DNA,⁶ these atoms are 3.7–3.8 Å apart. This backbone stretch is reflected in the torsional angle ζ of T3, which assumes a trans conformation.

Recently, a number of platinated oligonucleotide have been synthesized and investigated by NMR spectroscopy.^{4a,12} Since the kinked models have several features distinct from the unknicked one, such as the sugar conformation of C4, advanced NMR techniques should enable us to determine the predominant structure under a given set of conditions. Unfortunately, only rudimentary structural data on platinated double-stranded oligonucleotides have been reported thus far, and a detailed conformational analysis is still elusive. As far as modeling of platinated DNA is concerned, it should be pointed out that the kinked models better account for the well-known shortening and unwinding of superhelical DNA upon platination,¹³ whereas, in model A, only a slight shortening (by 1–1.5 Å/10 residues) and no significant unwinding of the B-DNA helix are indicated.

For a kinked $cis\text{-[Pt(NH}_3\text{)}_2\text{]}^{2+}$ -DNA adduct, the preference for either model B or C would clearly depend on ionic strength. Under low-salt conditions, the phosphate groups are expected to be fully hydrated, and bridging cations such as required for model B are

less likely. Accordingly, we believe that, with B, we have discovered a “high-salt model”, while C represents a “low-salt model” for kinked $cis\text{-[Pt(NH}_3\text{)}_2\text{]}^{2+}$ adducts of DNA.

While model A was stabilized by one ammine-phosphate hydrogen bond, the kinked models show two such hydrogen bonds. Recently, Sundaralingam constructed a framework model for a kinked oligonucleotide- $cis\text{-[Pt(NH}_3\text{)}_2\text{]}^{2+}$ adduct featuring one ammine-phosphate hydrogen bond to a phosphate group corresponding to p4 in the decanucleotide **2** considered in this work. In attempting to simulate this structure, we discovered another kinked model, featuring ammine-phosphate hydrogen bonds to both p4 and p3 phosphate groups. This model is currently being refined and will be discussed elsewhere.⁵

Acknowledgment. This work was supported by U.S. Public Health Service Grant CA34992 (to S.J.L.) awarded by the National Cancer Institute, Department of Health and Human Services. J.K. was supported by the Schweizerischer Nationalfonds zur Förderung der wissenschaftlichen Forschung.

Registry No. $cis\text{-[Pt(NH}_3\text{)}_2\text{]}-\text{[d(TCTCGGTCTC)-d(GAGACCGAGA)-N7(5),N7(6)]}\cdot 16\text{Na}$, 100102-29-2.

Supplementary Material Available: Listings of atomic coordinates for model B and model C structures of $cis\text{-[Pt(NH}_3\text{)}_2\text{]}-\text{[d(TCTCGGTCTC)-d(GAGACCGAGA)-N7(5),N7(6)]}$ (18 pages). Ordering information is given on any current masthead page.

(14) (a) Department of Chemistry. (b) Department of Biology.

Departments of Chemistry and Biology
Massachusetts Institute of Technology
Cambridge, Massachusetts 02139

Jiri Kozelka^{14a}
Gregory A. Petsko^{14a}
Gary J. Quigley^{14b}
Stephen J. Lippard^{14a}

(13) (a) Macquet, J.-P.; Butour, J.-L. *Biochimie* **1978**, *60*, 901–914. (b) Cohen, G. L.; Bauer, W. R.; Barton, J. K.; Lippard, S. J. *Science (Washington, D.C.)* **1979**, *303*, 1014–1016.